Effect of the Tie-Layer Thickness on the Delamination and Tensile Properties of Polypropylene/Tie-Layer/Nylon 6 Multilayers

D. Khariwala,[1] M. Ling,[2] A. Hiltner,[1] E. Baer[1]

[1]*Department of Macromolecular Science and Center for Layered Polymeric Systems, Case Western Reserve University, Cleveland, OH 44106*
[2]*Baxter Healthcare Corp., Round Lake, IL 60073*

ABSTRACT: This study examined the effect of the tie-layer thickness on the delamination behavior of polypropylene/tie-layer/nylon 6 multilayers. Various maleated polypropylene resins were compared for their effectiveness as tie-layers. Delamination failure occurred cohesively in all the multilayer systems. Two adhesion regimes were defined according to the change in the slope of the linear relationship between the delamination toughness and the tie-layer thickness. The measured delamination toughness of the various tie-layers was quantitatively correlated to the length of the damage zone that formed at the crack tip. In addition, the effect of the tie-layer thickness on the multilayer tensile properties was correlated with the delamination behavior. The fracture strain of the multilayers decreased with decreasing tie-layer thickness. An examination of the prefracture damage mechanism of the stretched multilayers revealed a good correlation with the delamination toughness of the tie-layers. In thick tie-layers (>2 μm), the delamination toughness was great enough to prevent the delamination of the multilayers when they were stretched. In thin tie-layers (<2 μm), the delamination toughness of all the tie-layers was low; consequently, delamination led to premature fracture in the stretched multilayers. © 2011 Wiley Periodicals, Inc. J Appl Polym Sci 121: 1999–2012, 2011

Key words: adhesion; coextrusion; damage zone; fatigue analysis; graft copolymers

INTRODUCTION

Typical multilayer barrier films for packaging applications involve structures in which the outer layers are polyolefins and the core layers consist of various polar polymers. Polyolefins, which are nonpolar by nature, serve as moisture barriers. However, they have relatively poor oxygen barrier characteristics. On the other hand, polar materials such as polyamides (PAs) have good oxygen and carbon dioxide barrier properties but show poor resistance to moisture. Therefore, a multilayer structure consisting of outer polyolefin layers with a core layer of an oxygen and carbon dioxide barrier polymer is a system that optimizes resistance to both moisture and gas.

Blends of polyolefins and PAs are incompatible over their entire composition ranges. Various compatibilization studies of polypropylene (PP)/PA blends using compatibilizer polymers have been reported.[1–4] A graft copolymer is usually used as a compatibilizing agent; the polymer consists of a polyolefin backbone grafted with functional groups such as maleic anhydride (MAH)[5–8] or acrylic acid.[9] In the case of maleic anhydride grafted polypropylene (MAH-*g*-PP), the anhydride groups react with the PA end groups and thereby form an *in situ* copolymer.[1] The remainder of the compatibilizer maintains its compatibility with the PP phase. In this manner, MAH-*g*-PP enhances adhesion in PP/PA blends.

A similar strategy has also been used to impart adhesion to layered structures by the incorporation of a graft copolymer tie-layer between the polyolefin and PA layers.[10–13] However, the mechanical performance of the final multilayer materials will be limited by the premature delamination of the multilayer structure. Hence, it is essential to provide adequate adhesion and to understand the variables that affect the adhesion between these types of polymer–polymer layered structures.

Previously, microlayer coextrusion was used to study adhesion in multilayers of PP and high-density polyethylene (HDPE) with elastomeric tie-

TABLE I
PP-Based Tie-Layer Resins

Resin grade	Supplier	Short code	MAH (wt %)[a]	MAH (wt %)[b]	Density (g/cm^3)	MFR at 230°C (g/10 min)
MAH-g-PP						
Polybond 3002	Chemtura	L-gPP	0.1	0.08	0.910	7
Orevac CA100	Arkema	H-gPP	1.1	0.5	0.910	150
MAH-g-PP filled with rubber particles (32 vol %)						
Orevac PPC	Arkema	R-gPP	0.2	—	0.890	2
MAH-grafted ethylene–propylene rubber						
Exxelor VA1803	Exxon	gEPR	1.1	0.4	0.860	3

[a] Provided by the supplier.
[b] Obtained by FTIR analysis at Dow Chemical Co.

layers.[14] Multilayer tapes of many alternating layers of PP and HDPE with individual tie-layer thicknesses on micrometer and nanometer scales were fabricated. T-peel tests provided the direct measurement of the delamination toughness provided by the tie-layers. It was found that the tie-layer thickness and the chain microstructure of the tie-layer material had significant effects on the delamination toughness. The dependence of the delamination toughness on the tie-layer thickness showed two regions.[15] Thin tie-layers less than 2 μm thick showed a much stronger dependence on the layer thickness than thicker tie-layers. An inspection of the crack-tip damage zone revealed that the mechanism changed from thicker tie-layers to thinner tie-layers.

In this article, the effect of the tie-layer thickness on the delamination toughness and delamination mechanism of PP/tie-layer/nylon 6 multilayers is studied. The delamination performance of various maleated PP tie-layer resins is also compared. In addition, the effect of the tie-layer thickness on the tensile properties of PP/tie-layer/nylon 6 multilayers is correlated with the delamination behavior.

EXPERIMENTAL

Two grades of PP and nylon 6 adherends were used in this study with various melt flow rates (MFRs). PPs with MFRs of 3 and 12 g/10 min at 230°C (H105-03NA and H700-12R, respectively) were obtained from Dow Chemical Co., Midland, MI. Nylon 6 grades with MFRs of 20 and 120 g/10 min at 275°C (FG40 and BS/2, respectively) were obtained from EMS, Sumter, SC. Four different maleated polymers were used as tie-layers (Table I). The MAH contents (wt %) according to the suppliers are listed in Table I. Two were maleated PPs with high and low MAH contents. Polybond 3002 (Chemtura) was lightly grafted with 0.08% MAH and was labeled L-gPP. Orevac CA100 (Arkema) had a higher amount of grafting (0.5% MAH) and was labeled H-gPP. A third material was maleated PP filled with ethylene–propylene rubber (Orevac PPC, Arkema),

which was labeled R-gPP; this material was lightly grafted (0.2% MAH). The last tie-layer resin was a maleated ethylene–propylene rubber (Exxelor VA1803, Exxon) with a higher amount of grafting (0.4% MAH), which was labeled gEPR.

Compression-molded sheets with a thickness of approximately 0.5 mm were prepared for thermal analysis and dynamic mechanical analysis. Pellets were sandwiched between Mylar sheets, preheated at 190°C under minimal pressure for 8 min, compressed at 10 MPa for 5 min in a laboratory press, and cooled at approximately 30°C/min with circulating cold water. Thermal analysis was performed with a PerkinElmer, Waltham, MA DSC-7 calorimeter under a nitrogen atmosphere. Specimens weighing 5–10 mg were cut from the molded sheets, and thermograms were obtained at a heating rate of 10°C/min from −60 to 190°C. Dynamic mechanical thermal analysis (DMTA) was carried out with a Polymer Laboratories MKII dynamic mechanical thermal analyzer. Specimens were tested in the dynamic tensile mode at a frequency of 1 Hz and at a strain of 0.1% from −60 to 120°C at a heating rate of 3°C/min with a grip-to-grip separation of 13 mm.

The stress–strain behavior of the tie-layer materials was measured with ASTM D 638 microtensile specimens cut from the compression-molded films. The tests were performed with an MTS Alliance, Eden Prairie, MN RT/30 testing machine. The separation of the grips was 22.3 mm, and the specimen width was 4.8 mm. The specimens were stretched at a strain rate of 100%/min at room temperature. The engineering stress and strain were calculated conventionally from the initial cross-section area and grip separation.

Multilayer tapes and films were coextruded with the three-component layer-multiplying process described previously.[16] The multilayer films consisted of alternating layers of PP and nylon 6 separated by a tie-layer. For the delamination study, multilayer tapes with 65 layers (17 PP layers and 16 nylon 6 layers separated by 32 layers of the tie-layer) were coextruded to produce tie-layer thicknesses

ranging from 2 to 20 μm. Very thin tie-layers ranging from 0.2 to 2 μm were produced with 257 layers (65 PP layers and 64 nylon 6 layers separated by 128 tie-layers). The tapes were approximately 2 mm thick and 12 mm wide. Different tie-layer thicknesses were produced by variations of the extruder feed ratios. The adherend PP and nylon 6 layers had a thickness of approximately 50 μm for multilayer tapes with 65 layers and a thickness of approximately 15 μm for tapes with 257 layers. A multilayer tape of PP and nylon 6 with no tie-layer was also produced as a control. All the tapes were collected on a conveyor-belt takeoff unit and were quenched in cold water. Multilayer films for the tensile study were coextruded with 9 layers with tie-layer thicknesses of 10 and 2.5 μm. Thinner tie-layer thicknesses of 0.6 and 0.3 μm were produced from 17-layer films. The films were 8 mil thick and 14 in. wide. Different tie-layer thicknesses were produced by variations of the extruder feed ratios. The adherend PP and nylon 6 layers had a thickness of approximately 50 μm for multilayer films with 9 layers and a thickness of approximately 25 μm for films with 17 layers. A multilayer film of PP and nylon 6 with no tie-layer was also produced as a control. All the tapes were quenched on a chill-roll takeoff unit. The R-gPP and gEPR tie-layers were coextruded with the low-MFR PP and nylon 6, and the L-gPP and H-gPP tie-layers were coextruded with the high-MFR PP and nylon 6. All the multilayer tapes and films were dried in a desiccator for at least 2 days before testing.

Delamination of the tapes was carried out with a modified T-peel test (ASTM D 1876). Strips 6.4 mm wide and 20 cm long were cut from the center of the microlayered tape and were notched with a fresh razor blade pushed into a tie-layer at the midplane of the tape. The notch was examined with an optical microscope to ensure that the crack started along a single interface. Tapes were subsequently loaded at 21°C in the MTS testing machine at a rate of 10 mm/min. The results of three tests are reported.

The composition of the matching peel surfaces of the tapes was determined with a Nicolet, Waltham, MA 800 Fourier transform infrared (FTIR) spectrometer in the attenuated total reflection (ATR) mode. Three different areas on each peel surface were tested. To study the damage zone ahead of the crack tip during delamination of the tapes, some peel specimens were polished and coated on the edges with 150 Å of gold before they were loaded into a tensile deformation stage and inserted into a JEOL, Peabody, MA JSM 6510LV scanning electron microscope. The specimens were peeled *in situ* at a rate of 0.2 mm/min.

The stress–strain behavior of the multilayer films was measured as described previously at a strain rate of 100%/min at 23°C. At least three specimens
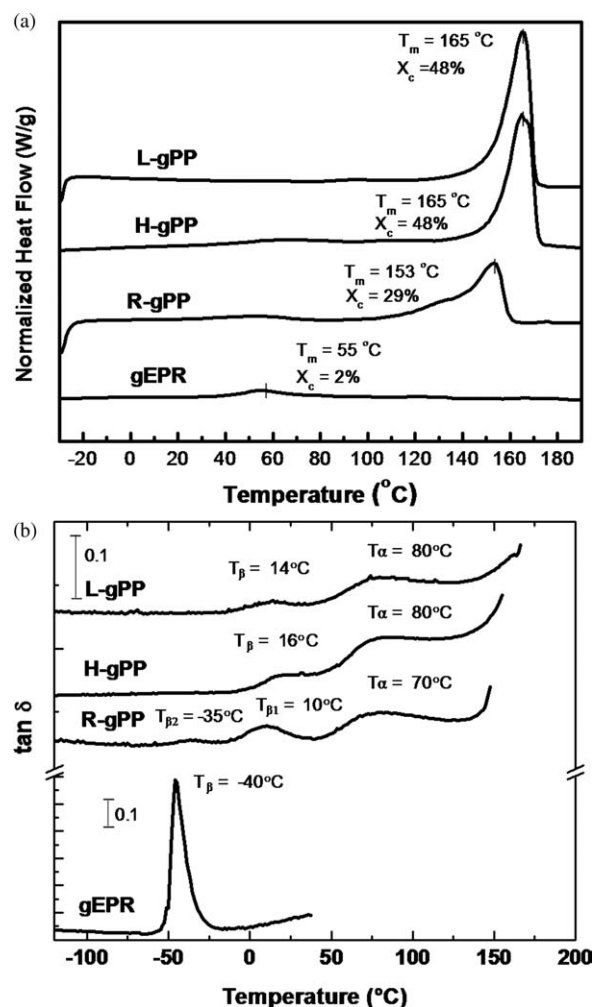
Figure 1 Comparison of the thermal behavior of all the tie-layer materials: (a) DSC (T_m = peak melting temperature, X_c = crystallinity) and (b) DMTA (T_α = peak α-relaxation temperature, T_β = peak β-relaxation temperature).

of each film were tested, and the data were averaged. The prefracture damage mechanism was examined by scanning electron microscopy (SEM) with specimens that had been stretched close to fracture. A small piece was cut from the stretched specimen and microtomed along the stretching direction at 23°C. The microtomed surface was coated with 150 Å of gold before it was examined by SEM.

RESULTS AND DISCUSSION

Characterization of the tie-layer resins

The thermal transitions of the tie-layer materials were characterized with differential scanning calorimetry (DSC) and DMTA. The DSC first-heating curves in Figure 1(a) show that L-gPP and H-gPP had a sharp melting point at 165°C similar to the melting point of isotactic PP. The crystallinity was calculated from the heat of melting with a value of 209

TABLE II
Properties of the Tie-Layer Resins

Tie-layer	Density (g/cm^3)	Peak melting temperature $(°C)$	Crystallinity (%)	2% secant modulus (MPa)	Yield stress (MPa)	Fracture strain (%)	Fracture stress (MPa)
L-gPP	0.910	165	48	830	35	270	22
H-gPP	0.910	165	48	830	33	11	30
R-gPP	0.890	153	29	300	23	490	27
gEPR	0.860	55	2	2.6	0.5	280	0.4

J/g for the heat of fusion of 100% crystalline isotactic PP (Table II).[17] The crystallinity of L-gPP and H-gPP was 48%. The rubber-filled tie-layer R-gPP had a broader and lower melting peak at 153°C. The presence of rubber particles decreased the crystallinity to 29%. gEPR had a small melting peak at 55°C with very low crystallinity. The glass-transition temperature (T_g) was taken from the DMTA tan δ curves in Figure 1(b). The β-relaxation peak corresponding to T_g was found at 15°C for L-gPP and H-gPP. For R-gPP, in addition to the β-relaxation peak at 10°C, an additional peak at −35°C was observed, and it probably corresponded to T_g of the rubber particles. All three materials also showed an α-relaxation temperature around 80°C that arose from the crystalline regions. gEPR showed a low β-relaxation temperature at −40°C. The high intensity of the β-relaxation peak and the absence of an α-relaxation peak reflected the very low crystallinity of gEPR. The atomic force microscopy cross-section image of R-gPP in Figure 2 shows that the material was filled with rubber particles (32 vol %) ranging in size from 0.2 to 2 μm. The delamination and tensile tests of the multilayers were carried out at room temperature between T_g and the peak melting temperature of the tie-layer materials.

Determination of the delamination interface of the peeled multilayer tapes

The failure location of the peeled multilayer tapes was identified from the composition of the peeled surfaces by ATR–FTIR. The adherends and adhesive tie-layers had unique FTIR peaks that allowed for their differentiation. The peeled surfaces of tapes without a tie-layer led to spectra that were identical to those of the PP and nylon 6 controls, and this indicated no adhesion between them. The spectra of the two surfaces from a peeled tape with 7-μm tie-layers, together with the spectra of nylon 6, PP, and tie-layer controls, are compared in Figure 3. Figure 3(a) shows a comparison of the tapes with an L-gPP tie-layer with only 0.08% MAH; one surface matched the L-gPP control, and the other closely matched nylon 6. However, the nylon 6 side also showed a peak at 2866 cm^{-1} and a shoulder at 2950 cm^{-1} (C—H stretching), which are indicated by arrows on the spectrum. This means that a tie-layer

was left on the nylon 6 surface. The results indicated that cohesive failure had occurred close to the nylon 6/tie-layer interface in the L-gPP tapes. In the H-gPP tie-layers, which had a higher graft content of 0.5% MAH, cohesive fracture was even clearer. In this case, the spectra of the two delaminated surfaces were identical to the spectrum of the tie-layer control [Fig. 3(b)]. The peak at 1790 cm^{-1} corresponded to the MAH graft in the tie-layer and was not present for the PP control. Similarly, the delamination mechanism for the R-gPP and gEPR tie-layers with MAH contents of 0.2 and 0.4%, respectively, was also identified as cohesive. Thus, the FTIR observations confirmed that the delamination of the tapes with all the tie-layers was cohesive.

Effect of the tie-layer thickness on the delamination toughness of the multilayer tapes

A microlayered tape was notched at one end with a razor blade driven into the adhesive layer. As the
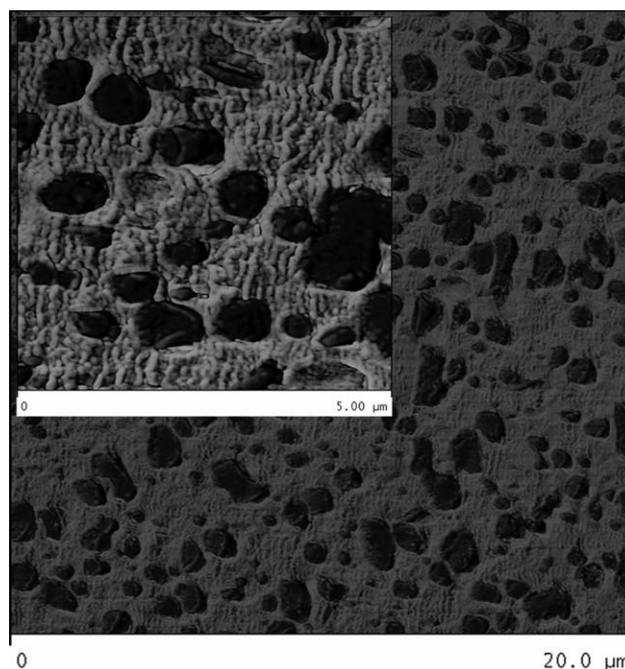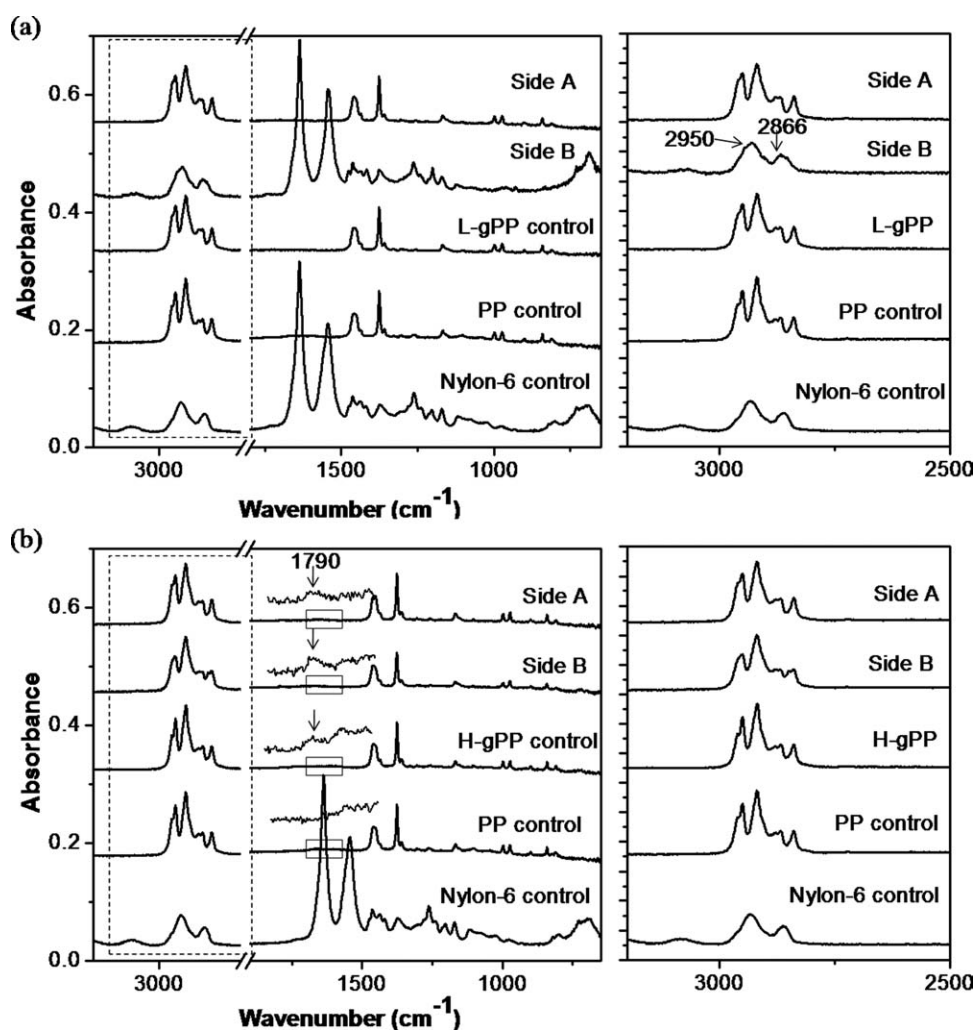

Figure 2 Atomic force microscopy phase morphology of an R-gPP cross section (scale = 20 μm). The inset shows a higher magnification image (scale = 5 μm).

Figure 3 FTIR identification of the peeled surface composition of multilayers with a tie-layer thickness of 7 μm: (a) L-gPP and (b) H-gPP. The spectra are magnified from 3200 to 2500 cm^{-1} on the right. The arrows in part a point to peaks from the tie-layer left over on the nylon 6 surface.

notched specimen was loaded, the arms were bent into a T-peel configuration until the crack started to propagate steadily at a constant load. The beam arms did not return to their original shape upon the removal of the load because of some plastic deformation of the beam arms. The delamination toughness (G) was measured as follows:

$$G = 2P/w \qquad (1)$$

where P is the load during steady crack propagation and w is the width of the specimen. The delamination toughness is plotted against the tie-layer thickness in Figure 4. Two regimes were defined according to the changes in the slope of the linear relationship between G and the tie-layer thickness. In the thick tie-layer regime (>2 μm), the G value of L-gPP and H-gPP was independent of the tie-layer thickness. This suggested that only a small amount of the tie-layer adjacent to the nylon 6/tie-layer

interface was deformed during peeling. G increased only slightly from 550 to 650 J/m^2 as the MAH graft content was increased from 0.08% in L-gPP to 0.5% in H-gPP. This indicated that increasing the MAH content did not substantially enhance G, and even a small amount of MAH in the tie-layers was sufficient to provide good adhesion to nylon 6. In the same regime, the G value of R-gPP was substantially higher than the value of all the other tie-layers, and it increased linearly with the tie-layer thickness. This suggested that the energy was absorbed by deformation of the entire tie-layer. gEPR showed the lowest G value in this regime, and it also increased linearly with the tie-layer thickness; this suggested that in this case also the energy was absorbed by deformation of the entire tie-layer. In the thin tie-layer regime (<2 to 3 μm), G decreased rapidly with decreasing tie-layer thickness for all the tie-layers. Two analogous regimes based on the tie-layer thickness were also observed in PP/HDPE microlayers
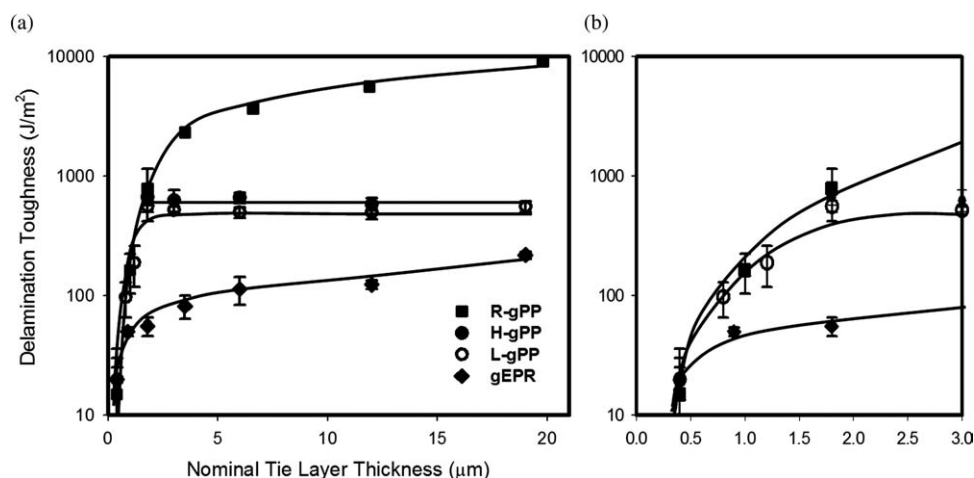
Figure 4 Effect of the tie-layer thickness on the delamination toughness: (a) the entire range of studied tie-layer thicknesses and (b) a magnified plot of the results for thinner tie-layers. The crosshead speed was 10 mm/min, and the temperature was 23°C.

with elastomeric tie-layers.[18,19] In these cases, the transition from the thick tie-layer regime to the thin tie-layer regime also occurred around 1–2 μm

Delamination mechanism of the peeled multilayer tapes

The damage zone at the peel crack tip was observed *in situ* by SEM. The damage zone images of tapes with L-gPP tie-layers are shown in Figure 5. In the thick tie-layer regime (>2 μm), the damage zone appeared to be localized at the nylon 6/tie-layer interface. The remainder of the tie-layer remained undeformed. After final separation at the nylon 6/tie-layer interface, the deformed material in the tie-layer did not recover completely but underwent substantial irreversible deformation. The behavior was consistent with localized plastic yielding of the tie-layer. All the thick L-gPP tie-layers formed a well-defined yield zone [Fig. 5(a,b)]. The damage zone length of L-gPP did not depend strongly on the tie-layer thickness, and this was consistent with localized deformation of the tie-layer at the nylon 6/tie-layer interface. As the thickness was reduced, more of the tie-layer was incorporated into the yield zone until there was not enough material to support a continuous yield zone, and the material broke up into fibrils. The fibrillated damage zone observed in the thin tie-layer regime (<2 μm) was 75–80% void space [Fig. 5(c,d)]. As a result, the delamination toughness was considerably reduced in the thinner tie-layers. The damage zones of L-gPP and H-gPP are compared in Figure 5(e,f). The SEM images clearly show that the damage zone was still localized at the nylon 6/tie-layer interface in the H-gPP tie-layers. A small amount of the tie-layer adjacent to the interface yielded with the formation of highly

stretched fibrils. The remainder of the tie-layer remained undeformed. The damage zone length of H-gPP was longer than that of L-gPP.

The damage zone at the crack tip for the R-gPP tie-layer is shown in Figure 6. In the thick tie-layer regime [Fig. 6(a,b)], R-gPP appeared to deform entirely into a highly fibrillated and long damage zone, in contrast to the localized tie-layer deformation seen in L-gPP and H-gPP tie-layers. Consequently, the damage zone length and crack tip opening for R-gPP were much larger than those for L-gPP and H-gPP. It seems that the formation of the fibrillate damage zone in the tie-layer was enabled by rubber particle cavitation in a manner similar to that for rubber-toughened polymers.[20–22] The holes at the crack tip of the R-gPP tie-layer were probably formed by rubber cavitation. In addition, the damage zone length and the crack tip opening decreased with decreasing tie-layer thickness, and this was consistent with deformation of the entire tie-layer thickness. As the R-gPP tie-layer thickness further decreased into the thin tie-layer regime (<2 μm), the damage zone length decreased further, and only very short fibrils were visible [Fig. 6(c,d)]. In the thin tie-layer regime, the layer thickness approached the size of the individual rubber particles, and the rubber probably did not effectively fibrillate the entire tie-layer. Consequently, the delamination toughness decreased rapidly in the thin tie-layers.

The damage zone at the crack tip for the elastomeric gEPR tie-layers is shown in Figure 7. In the thick tie-layer regime [Fig. 7(a,b)], the tie-layer entirely deformed into a well-defined, continuous damage zone. After failure, the tie-layer substantially recovered because of its elastomeric nature. As the tie-layer thickness decreased from 19 to 7 μm, the damage zone length and crack-tip opening
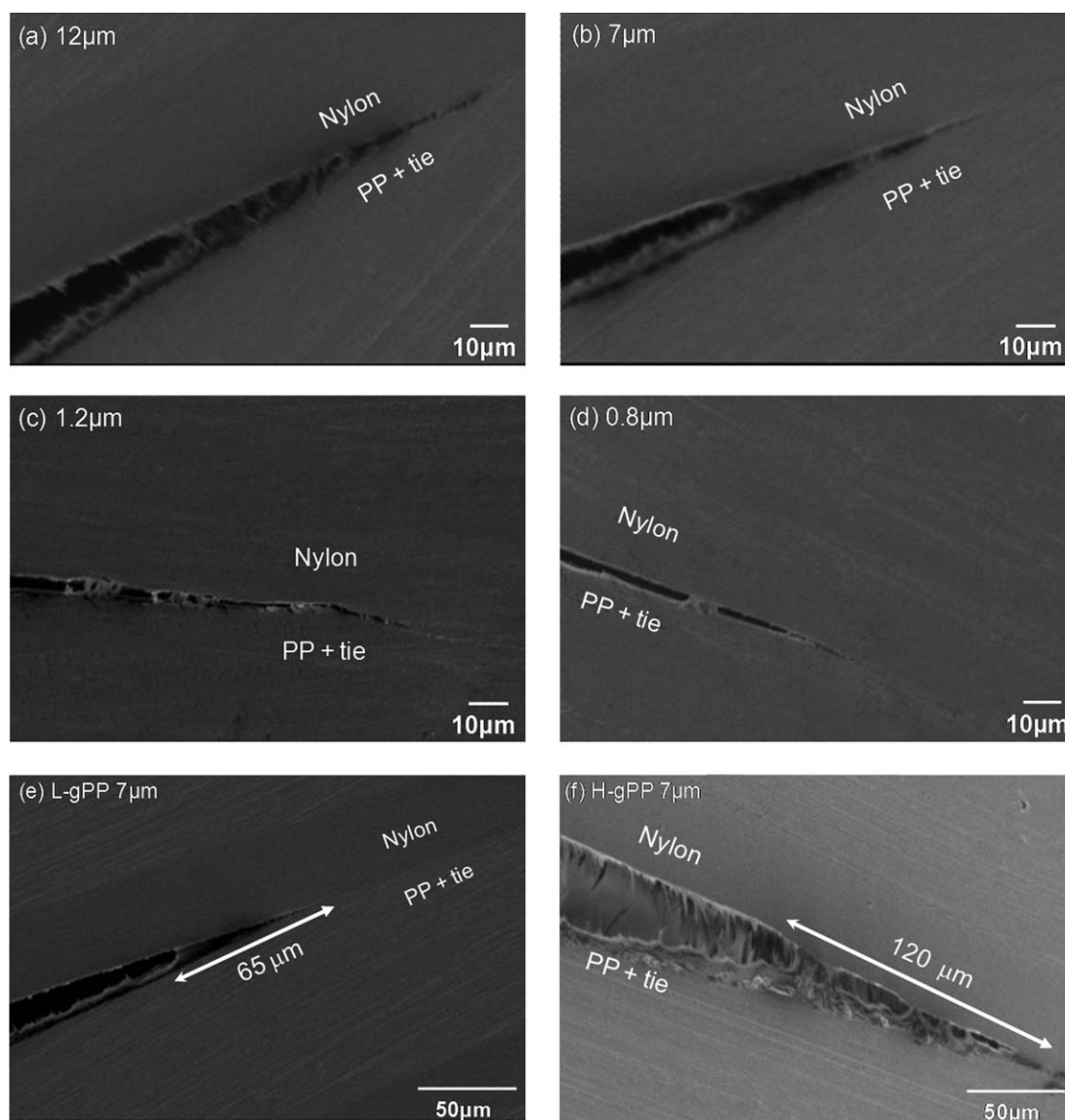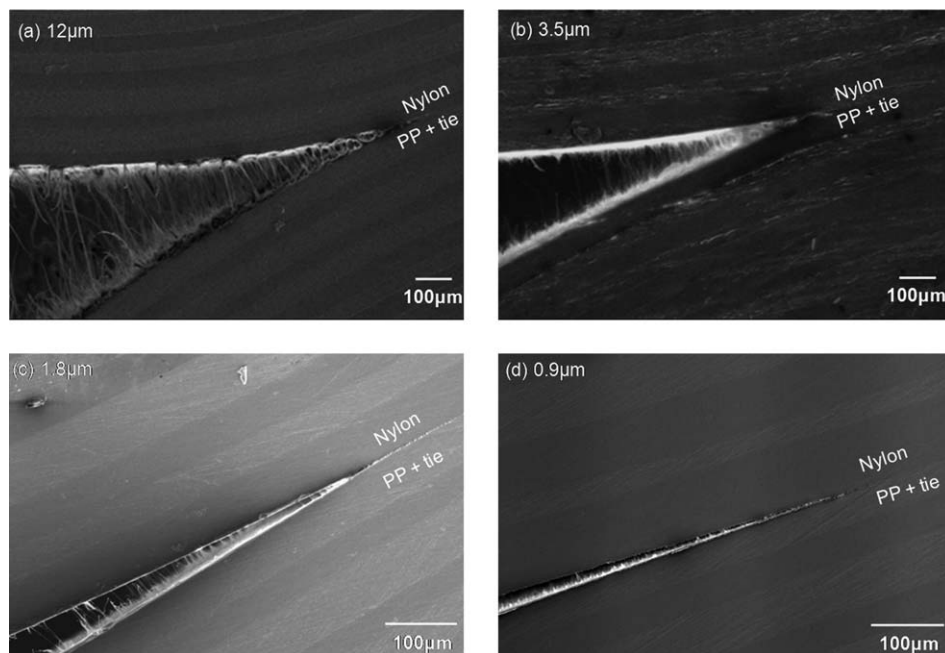
Figure 5 SEM images from an *in situ* peel test showing the effect of the tie-layer thickness on the L-gPP damage zone [(a) 12, (b) 7, (c) 1.2, and (d) 0.8 μm] and the effect of the MAH content on the damage zone of 7-μm tie-layers [(e) L-gPP and (f) H-gPP].

decreased, and this was consistent with deformation of the entire tie-layer. As the gEPR tie-layer thickness further decreased into the thin tie-layer regime (<2 μm), the continuous damage zone was replaced with a highly fibrillated craze zone with 65–75% void space separating the load-bearing fibrils [Fig. 7(c,d)]. In the very thin tie-layers, there was not enough material to support a continuous damage zone, and the material broke up into fibrils. Consequently, the delamination toughness decreased rapidly in the thin regime.

The damage zones of all the tie-layers are compared schematically in Figure 8. The schematics on the left represent the thick tie-layers (>2 μm), and those on the right represent the thin layers (<2 μm). In the thick tie-layer regime, L-gPP and H-gPP exhibited a localized yield zone, and the rest of the

tie-layer remained undeformed. In contrast, in the R-gPP tie-layer, the rubber particles enabled complete deformation of the tie-layer into a long, fibrillated damage zone. Because of its elastomeric nature, the gEPR tie-layer formed a continuous damage zone through deformation of the entire tie-layer. In the thin tie-layer regime, a fibrillated damage zone was observed for all the tie-layers. In the L-gPP and gEPR tie-layers, when the tie-layer was thinner than 2 μm, it did not contain enough material to produce the damage zone observed in thick tie-layers. Both the localized yield zone in L-gPP and the continuous damage zone in gEPR were replaced with a fibrillated craze that consumed the entire tie-layer. In thin R-gPP tie-layers, the rubber particles probably did not effectively fibrillate the entire tie-layer, and a damage zone consisting of very short fibrils was
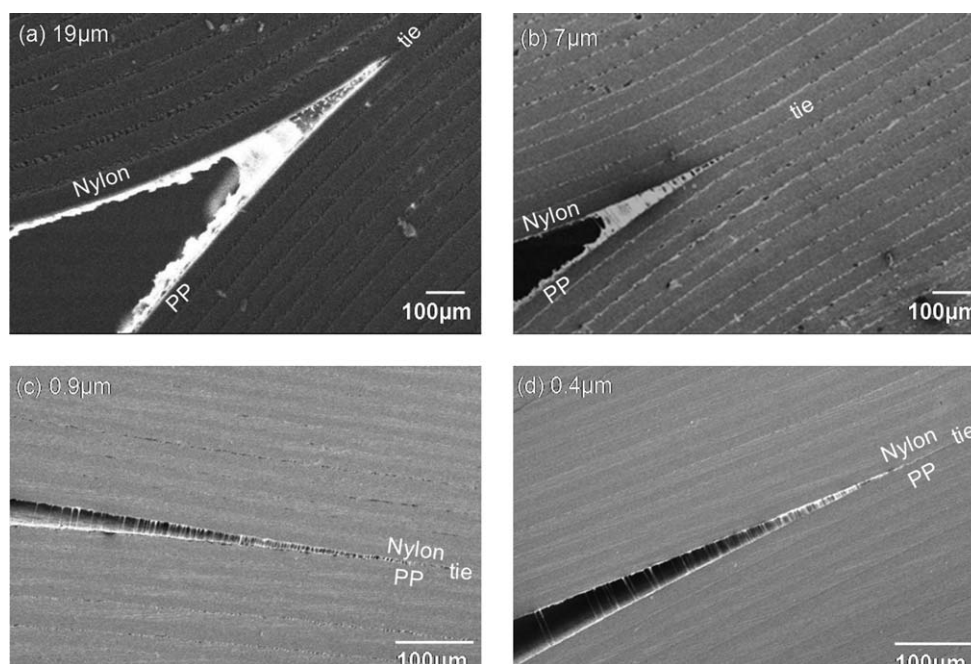
Figure 6 SEM images from an *in situ* peel test showing the effect of the tie-layer thickness on the R-gPP damage zone: (a) 12, (b) 3.5, (c) 1.8, and (d) 0.9 μm.

observed. The fibrillated zone was similar to that observed in the L-gPP tie-layer.

### Damage zone analysis of the multilayer tapes

In the peel test, the delamination toughness generally receives contributions from tie-layer deformation, beam-arm deformation, and interfacial adhesive failure. The beam-arm deformation includes bending and stretching. In similar peel tests using micro-layered tapes, contributions from both bending and stretching were found to be within the experimental error and could be neglected.[23] Because the failure mechanism of the tie-layers was cohesive, G was mainly due to the energy-absorbing tie-layer deformation.

Figure 7 SEM images from an *in situ* peel test showing the effect of the tie-layer thickness on the gEPR damage zone: (a) 19, (b) 7, (c) 0.9, and (d) 0.4 μm.
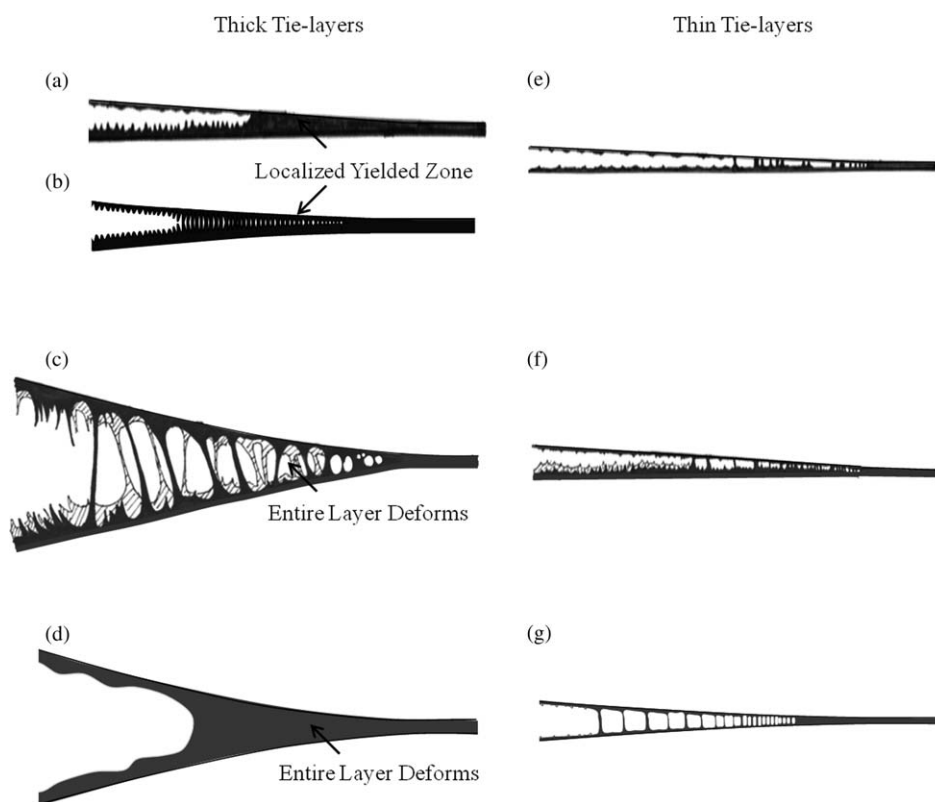
Figure 8 Schematic comparison of the tie-layer damage zones in the thick regime (>2 μm) on the left and in the thin regime (<2 μm) on the right: (a,e) L-gPP, (b) H-gPP, (c,f) R-gPP, and (d,g) gEPR.

The delamination toughness can be analyzed if we consider the damage zone as an Irwin plastic zone. If we assume that only the tie-layer undergoes plastic deformation with the formation of a damage zone of length a at the crack tip, the delamination toughness can be calculated as follows:[24,25]

$$G_p = \frac{2\pi a \sigma_{dz}^2}{E} \quad (2)$$

where Gp is the calculated delamination toughness and sdz is the stress state of the tie-layer inside the damage zone and E is the tensile modulus of the tie-layer. L-gPP and H-gPP tie-layers showed only a localized yield zone, so σ_{dz} was taken to be the yield stress. In R-gPP and gEPR tie-layers, the entire tie-layer deformed, so σ_{dz} was taken to be the stress at break. When the damage zone is highly voided, the damage zone length (i.e., a) is replaced with an effective damage zone length (a_f), which considers only the fraction of the damage zone length supported by the load-bearing fibrils:

$$G_{pf} = \frac{2\pi a_f \sigma_{dz}^2}{E} \quad (3)$$

where Gpf is the calculated delamination toughness of the fibrallated damage zone and af is obtained by the subtraction of the voided length from the total damage zone length.

The values of the yield stress, stress at break, and modulus were taken from constrained uniaxial tensile tests that simulated the deformation of the tie-
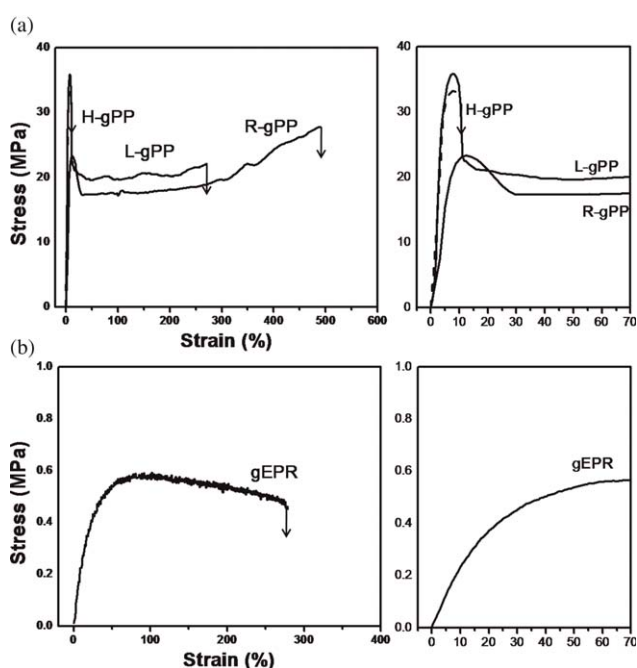
Figure 9 Stress–strain curves of the tie-layer materials: (a) L-gPP, H-gPP, and R-gPP and (b) gEPR.

TABLE III
Comparison of the Calculated and Measured G Values
of the L-gPP and H-gPP Tie-Layers

Tie-layer thickness (μm)	a (μm)	a_f (μm)	G (J/m^2)	
			Calculated	Measured
L-gPP tie-layers				
19	55	—	500	560 ± 60
12	70	—	630	510 ± 70
7	65	—	590	520 ± 50
3.5	60	—	540	520 ± 40
1.8	61	—	550	560 ± 60
1.2	80	17	150	190 ± 70
0.8	44	8	70	100 ± 30
H-gPP tie-layers				
7	121	105	650	660 ± 70

layer in the peel test (Fig. 9). L-gPP exhibited stress–strain behavior typical of that seen in semicrystalline thermoplastics with a high modulus, a sharp yield, cold drawing, and slight strain hardening. As expected, H-gPP also displayed a high modulus and a sharp yield but did not show any drawing, probably because of its very low molecular weight (MFR = 150) in comparison with L-gPP (MFR = 7). The presence of rubber particles in R-gPP significantly enhanced the toughness by increasing the strain hardening up to 500%. In addition, as we expected, the rubber also decreased the modulus and yield stress and broadened the yielding. gEPR behaved like an elastomer with uniform deformation and large strain recovery after fracture. However, its very low crystallinity was responsible for its very low stress response. The tensile properties of the tie-layer materials are listed in Table II.

The values of G_p and G_{pf} from eqs. (2) and (3) compared well with experimental values of G measured from peel tests for all the tie-layers in Tables III and IV. Table III shows a comparison for the L-gPP tie-layer. The agreement between the calculated and measured G values was found to be quite good at all tie-layer thicknesses. For the H-gPP tie-layer, the fraction of the damage zone length that was spanned by load-bearing fibrils was estimated from Figure 7(b) to be 0.65. Therefore, in the thick-layer regime, a_f was equal to 0.65a. The agreement between G_{pf} and G held even for the H-gPP tie-layer (Table III). In the thick regime, the slightly higher a_f value of H-gPP versus L-gPP was responsible for the somewhat higher G value. Table IV shows that the agreement between the calculated and measured G values extended even to R-gPP and gEPR tie-layers at all thicknesses. In thick R-gPP tie-layers, the rubber particles enabled the deformation of the entire tie-layer; hence, a greater damage zone length was obtained in comparison with L-gPP and H-gPP. Consequently, this tie-layer showed the highest G value in

the thick regime. A larger damage zone was also obtained in thick gEPR tie-layers versus L-gPP and H-gPP because of deformation of the entire elastomeric tie-layer. However, in the thick regime, its G value was lowest because of its very low modulus and stress at break.

Effect of the tie-layer thickness on the tensile properties of the multilayer films
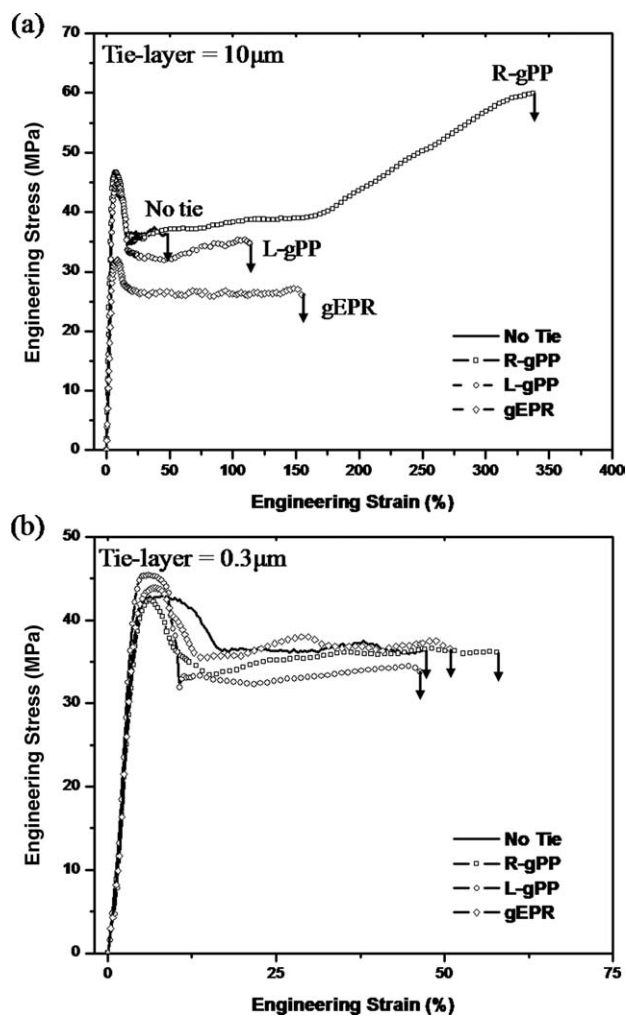
It is now interesting to understand the effect of the tie-layer thickness on the tensile behavior of the multilayers and to correlate it with the delamination behavior. The effect of the tie-layer thickness on the tensile behavior of the multilayer films is shown in Figure 10. The 2% secant modulus of the multilayer films at low strains is reported in Table V and is compared to the expected modulus of the multilayer from an additive relationship using the following equation:[26]

$$E_{\text{expected}} = \phi_{PP}E_{PP} + \phi_{\text{Nylon}}E_{\text{Nylon}} + \phi_{\text{tie}}E_{\text{tie}} \quad (4)$$

where E_{expected} is the expected modulus, ϕ is the volume fraction, and E is the modulus of the material. In the control without a tie-layer, the measured modulus compared well with the expected modulus from additivity. Also, with the thick and thin tie-layers, the measured moduli of the multilayer film were in close agreement with the expected modulus for all the tie-layers. At higher strains, all the multilayer films exhibited a stress–strain curve with yielding and neck propagation, and the tie-layer thickness predominantly affected the fracture strain (Table V). The control without any tie-layer fractured after the yield point during neck propagation

TABLE IV
Comparison of the Calculated and Measured G Values
of the R-gPP and gEPR Tie-Layers

Tie-layer thickness (μm)	a (μm)	a_f (μm)	G (J/m^2)	
			Calculated	Measured
R-gPP tie-layers				
19	1200	600	7900	9100 ± 560
12	1050	400	5300	5660 ± 280
7	590	265	3470	3700 ± 310
3.5	350	175	2290	2340 ± 100
1.8	250	52	690	790 ± 370
0.9	175	16	210	160 ± 60
gEPR tie-layers				
19	515	—	210	220 ± 15
12	410	—	165	125 ± 10
7	320	—	125	115 ± 30
3.5	200	—	80	80 ± 15
1.8	150	—	60	60 ± 10
0.9	400	100	40	50 ± 5
0.4	300	74	30	20 ± 10

Figure 10 Effect of the tie-layer thickness on the stress–strain curves of PP/tie/nylon 66 multilayer films at a strain rate of 100%/min at 23°C: (a) 10 and (b) 0.3 μm.

at 50% strain. Multilayers with thick tie-layers of 10 μm showed the maximum fracture strain [Fig. 10(a)]. The multilayer with R-gPP fractured after considerable strain hardening, whereas the multilayer with the L-gPP tie-layer fractured after some strain hardening, and the multilayer with gEPR fractured during neck propagation. When the tie-layer thickness was reduced to 2.5 μm, the fracture strain of the multilayers with L-gPP and gEPR tie-layers decreased and were only slightly higher than the control value. The fracture strain of the multilayer with R-gPP remained unaffected. Multilayers with tie-layers thinner than 2 μm showed poor tensile properties. Multilayers with L-gPP and gEPR tie-layers of 0.6 μm had the same fracture strain as the control (50% strain), and the multilayer with the R-gPP tie-layer fractured at a somewhat higher strain of 150%. When the tie-layers were further reduced to 0.3 μm, all the multilayers fractured at the same strain as the control [Fig. 10(b)].

Damage mechanism of the stretched multilayer films

The prefracture damage mechanisms were examined in the necked region by SEM with specimens that had been stretched close to fracture. Figure 11 shows a comparison of the prefracture mechanisms of multilayer films in the thick and thin tie-layer regimes. In the thick tie-layers (10 μm), there was no indication of delamination between the layers before fracture. The tie-layers provided good adhesion between PP and nylon, and the cracks were initiated within the tie-layer [Fig. 11(a-c)]. The fracture strain of the multilayer, therefore, depended on the fracture

TABLE V
Modulus and Fracture Strain Values of Multilayer Films with Various Tie-Layer Thicknesses

	10-μm tie layer			2.5-μm tie layer		
	Modulus (MPa)			Modulus (MPa)		
Multilayer film	Measured	Expected	Fracture strain (%)	Measured	Expected	Fracture strain (%)
PP/nylon 6 (no tie)	1150 ± 70	1160	50 ± 4			
PP/R-gPP/nylon 6	1000 ± 40	990	320 ± 20	1090 ± 120	1120	320 ± 20
PP/L-gPP/nylon 6	1030 ± 20	1130	120 ± 30	1090 ± 20	1150	60 ± 10
P/gEPR/nylon 6	890 ± 60	930	170 ± 30	1050 ± 40	1100	70 ± 10
	0.6-μm tie layer			0.3-μm tie layer		
	Modulus (MPa)			Modulus (MPa)		
Multilayer film	Measured	Expected	Fracture strain (%)	Measured	Expected	Fracture strain (%)
PP/R-gPP/nylon 6	1020 ± 50	1080	110 ± 10	1150 ± 30	1140	55 ± 10
PP/L-gPP/nylon 6	1160 ± 30	1150	50 ± 5	1100 ± 60	1160	50 ± 4
PP/gEPR/nylon 6	1040 ± 70	1060	50 ± 3	1090 ± 40	1130	50 ± 5
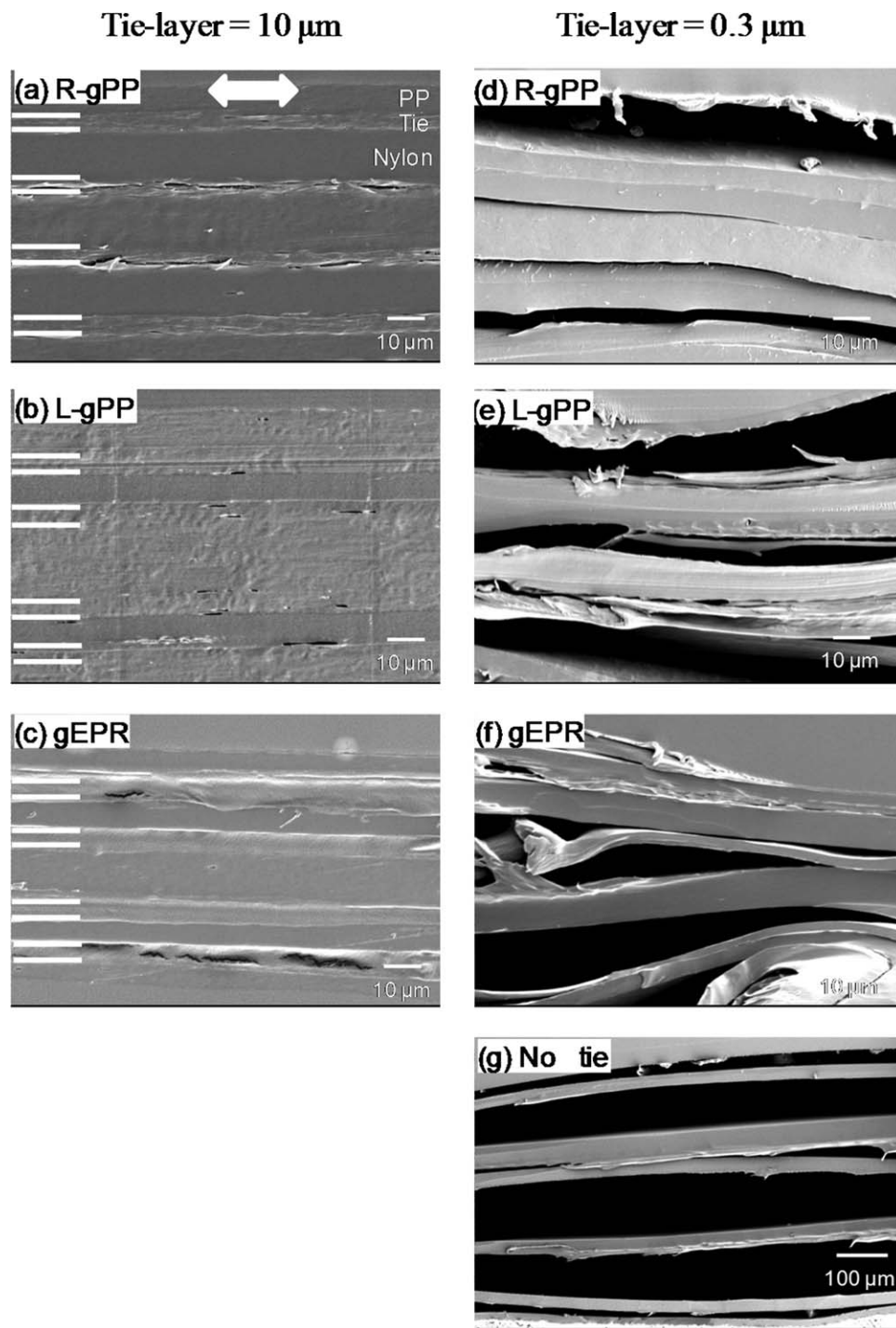
Figure 11 SEM images showing the effect of the tie-layer thickness on the deformation mechanism of PP/tie/nylon 66 multilayer films stretched close to fracture: (a–c) multilayers with a 10-μm tie-layer (markers on the left have been drawn to differentiate the tie-layers), (d–f) multilayers with a 0.3-μm tie-layer, and (g) a multilayer control with no tie-layer. The arrow in part a indicates the stretching direction for all the samples.

strain of the tie-layer material, as shown in Figure 11. When the tie-layer thickness was reduced to 2.5 μm, the multilayers with R-gPP and L-gPP tie-layers displayed good adhesion, with cracks again appearing only in the tie-layer before fracture. However, the multilayers with gEPR showed delamination before fracture, and this indicated that the adhesion between layers was not strong enough. In all the multilayers with tie-layers thinner than 2 μm, delamination preceded fracture; this reflected the poor adhesion that

was provided by all the tie-layers in this thickness range [Fig. 11(d–f)], and the damage mechanism was similar to that of the control [Fig. 11(g)].

Correlation between the delamination toughness and the tensile properties of the multilayers

It is now interesting to correlate the effect of the tie-layer thickness on the peel strength as studied in multilayer tapes to the tensile performance of multilayer films. The control without a tie-layer had almost no delamination toughness; consequently, the control multilayer films showed poor tensile fracture strain. In thick, 10-µm tie-layers, the delamination toughness was great enough that the tie-layers provided good adhesion in the multilayer films. Consequently, during tensile deformation of the multilayer films with all the tie-layers, no delamination was observed before fracture. The R-gPP material, which had the highest toughness of the tie-layer materials, produced the best multilayer tensile toughness. At the tie-layer thickness of 2.5 µm, the delamination toughness of gEPR was least. When the multilayer films with a 2.5-µm tie-layer thickness were stretched, the adhesion provided by the gEPR tie-layer was not great enough to prevent delamination before fracture. Consequently, the fracture strain in the multilayers with a 2.5-µm gEPR tie-layer was lower than that in the films with 10-µm gEPR tie-layers. R-gPP and L-gPP tie-layers of 2.5 µm provided enough adhesion to prevent delamination before fracture in the multilayer films. In the tie-layers thinner than 2 µm, the delamination toughness dropped rapidly for all the tie-layers. The tensile properties also deteriorated rapidly in this thin regime. Delamination led to premature fracture, and the fracture strain approached that of the control as the tie-layer thickness decreased. In the multilayers with the thinnest tie-layer thickness of 0.3 µm, the fracture strain was the same as that of the control for all the tie-layers.

CONCLUSIONS

This study examined the effect of the tie-layer thickness on the delamination behavior of PP/tie-layer/nylon 6 multilayers. In addition, the effect of the tie-layer thickness on the multilayer tensile properties was correlated with the delamination behavior. Various maleated PP resins were compared as tie-layers. Delamination failure occurred cohesively in all the multilayer systems. Two adhesion regimes were defined according to the changes in the slope of the linear relationship between the delamination toughness and the tie-layer thickness. In the thick tie-layer regime (>2 µm), the delamination toughness of the R-gPP tie-layers was substantially higher than that of the other tie-layers, and it increased linearly with the tie-layer thickness. Direct observation of the crack tip confirmed that energy was absorbed by deformation of the entire R-gPP tie-layer, which was enabled by the rubber particles. In the same regime, the delamination toughness of the L-gPP and H-gPP tie-layers was independent of the tie-layer thickness, and increasing the MAH content did not significantly increase the delamination toughness. In these tie-layers, only a small amount of the tie-layer adjacent to the nylon 6/tie-layer interface yielded and deformed during peeling. The delamination toughness of the thick elastomeric gEPR tie-layers was least but showed dependence on the tie-layer thickness. The crack tip showed that the entire tie-layer deformation absorbed the energy; however, its poor mechanical properties were responsible for its low delamination toughness. The thin (<2 µm) tie-layer regime coincided with a transition to a highly fibrillated damage zone and a stronger dependence of the delamination toughness on the thickness for all the tie-layers. The tie-layer thickness also affected the tensile properties of the multilayers (mainly the fracture strain). An examination of the prefracture damage mechanism of the stretched multilayers revealed a good correlation with the delamination toughness of the tie-layers. In thick tie-layers (>2 µm), the delamination toughness provided by the tie-layers was high enough to prevent the delamination of multilayers when they were stretched; hence, the fracture strain was much higher than that of the multilayer with no tie-layer. In thin tie-layers (<2 µm), the delamination toughness of all the tie-layers dropped to very low values; consequently, delamination preceded fracture in the stretched multilayers for all the tie-layers. The fracture strain decreased to that observed in the multilayers with no tie-layer.

References

1. Ide, F.; Hasegawa, A. J Appl Polym Sci 1974, 18, 963.
2. Duvall, J.; Sellitti, C.; Myers, C.; Hiltner, A.; Baer, E. J Appl Polym Sci 1994, 52, 195.
3. Seo, Y.; Ninh, T. H. Polymer 2004, 45, 8573.
4. Agrawal, P.; Oliveira, S. I.; Araujo, E. M.; Melo, T. J. A. J Mater Sci 2007, 42, 5007.
5. Okada, O.; Keskkula, H.; Paul, D. R. Polymer 2001, 42, 8715.
6. Sathe, S. N.; Surekha, D.; Srinivasarao, G. S.; Rao, K. V. J Appl Polym Sci 1996, 61, 97.
7. Sacchi, A.; Di Landro, L.; Pegoraro, M.; Severini, F. Eur Polym J 2004, 40, 1705.
8. Gaylord, N. J Polym Sci Polym Lett Ed 1982, 20, 481.
9. Sanchez-Valdes, S.; Flores-Gallardo, S. G.; Ramos De Valle, L. F.; Medellin-Rodriguez, F. J. J Adhes Sci Technol 2003, 17, 1815.

10. Pucci, M.; Jachec, K.; Machonis, J.; Shida, M. J Plast Film Sheet 1991, 7, 24.

11. Ebeling, T.; Norek, S.; Hasan, A.; Hiltner, A.; Baer, E. J Appl Polym Sci 1999, 71, 1461.

12. Cole, P. J.; Macosko, C. W. J Plast Film Sheet 2000, 16, 213.

13. Kamykowski, G. W. J Plast Film Sheet 2000, 16, 237.

14. Dias, P.; Lin, Y. J.; Poon, B.; Chen, H. Y.; Hiltner, A.; Baer, E. Polymer 2008, 49, 2937.

15. Ayyer, R. K.; Kamdar, A. R.; Lin, Y. J.; Dias, P. S.; Poon, B. C.; Hiltner, A.; Baer, E. Annu Tech Conf Soc Plast Eng Conf Proc 2009, 67, 428.

16. Bernal-Lara, T. E.; Ranade, A.; Hiltner, A.; Baer, E. In Mechanical Properties of Polymers Based on Nanostructure and Morphology; Michler, G. H., Balta Calleja, F. J., Eds.; CRC: Boca Raton, FL, 2005; p 629.

17. Brandrup, J.; Immergut, E. H. Polymer Handbook, 3rd ed.; Wiley: New York, 1989.

18. Kamdar, A. R.; Ayyer, R. K.; Poon, B. C.; Marchand, G. R.; Hiltner, A.; Baer, E. Polymer 2009, 50, 3319.

19. Lin, Y. J.; Poon, B. C.; Marchand, G. R.; Hiltner, A.; Baer, E. Polym Eng Sci 2010, 50, 592.

20. Partridge, I. K. In Multicomponent Polymer Systems; Miles, I. S., Rostami, S., Eds.; Longman Scientific & Technical: Essex, England, 1992; p 149.

21. Chou, C. J.; Vijayan, K.; Kirby, D.; Hiltner, A.; Baer, E. J Mater Sci 1988, 23, 2521.

22. Perkins, W. G. Polym Eng Sci 1999, 39, 2445.

23. Ronesi, V.; Cheung, Y. W.; Hiltner, A.; Baer, E. J Appl Polym Sci 2003, 89, 153.

24. Dillard, D. A. In The Mechanics of Adhesion; Dillard, D. A., Pocius, A. V., Eds.; Adhesion Science and Engineering I; Elsevier: Amsterdam, 2002; p 1.

25. Kinloch, A. J.; Young, R. J. Fracture Behavior of Polymers; Applied Science: Essex, England, 1983; p 74.

26. Schrenk, W. J.; Alfrey, T. Polym Eng Sci 1969, 9, 393.